

Vibro-impact NES: Nonlinear mode approximation using the multiple scales method

Balkis Youssef and Remco I. Leine

Institute for Nonlinear Mechanics, University of Stuttgart, Stuttgart, Germany,
youssef@inm.uni-stuttgart.de,
home page: <https://www.inm.uni-stuttgart.de/>

Abstract. The aim of the paper is to derive a *closed-form* approximation for a nonlinear mode of a system with a vibro-impact nonlinear energy sink. Hereto, the multiple scales method is used to analyze the dynamical behavior of a linear oscillator coupled with a vibro-impact nonlinear energy sink (VI NES). The steady state response in the vicinity of 1:1 resonance is approximated. The resonance frequency of the examined nonlinear system for different excitation levels is estimated and the corresponding backbone curve is identified. The theoretical findings agree with the simulation results and represent a possible new approach for system identification.

Keywords: Vibro-impact NES, nonlinear modes, system identification, backbone curve

1 Introduction

The present study investigates the dynamics of a strongly nonlinear system, comprising a linear oscillator (LO) with an embedded strong nonlinear attachment, i.e. a vibro-impact nonlinear energy sink (VI NES). The addition of a NES to primary structures helps absorb and mitigate the vibration energy when the structure is excited within a certain frequency range. Different types of coupling have been widely studied theoretically [5, 8, 10] and experimentally [9, 11, 13] in order to understand the essential changes in the dynamics of the whole system caused by such an attachment. A main phenomenon that has been observed for various types of NES is the irreversible targeted energy transfer (TET) that guarantees the absorption of the vibration energy from the primary structure. Many studies (e.g. [4, 5]) have been conducted to understand the working principle of NES, being strongly related to the theory of nonlinear modes (NM). Various numerical approaches, including control-based methods (e.g. [2, 15]), have been applied to approximate NMs of nonlinear vibrating structures through the approximation of periodic solutions of the corresponding conservative system. These methods are mainly based on Rosenberg's definition for NMs and on the invariance property of the NM in the configuration space under the system's flow [1]. Most of these studies use an asymptotic approach, i.e. the multiple scales method (MSM), to approximate the invariant manifold. This approach provides

a way to construct an approximation of the periodic solutions which depend simultaneously on different time scales as well as the invariant manifold, whose topology offers a valuable insight into the system behaviour [12, 13].

In this work, the simplest case of periodic motion of the vibro-impact NES is considered, namely 1:1 resonance with 2 symmetric impacts per period. The method of multiple scales is applied as in [5, 7] to approximate the solutions and determine a qualitative relation between the LO motion and the NES described by the slow invariant manifold (SIM). The SIM represents the set of all possible equilibria in the vicinity of 1:1 resonance and is therefore relevant in the study of TET. Based on these results, a closed-form expression for the backbone curve is identified. In this context, the backbone curve is defined as the curve connecting the maxima of the frequency response functions for different excitation levels [2, 14, 15]. The numerical simulation results of the backbone curve identification as well as the relevant findings are discussed.

2 Model description

The mechanical system is composed of a primary damped linear oscillator (LO) of mass M and a VI NES, built as a particle of mass m , moving freely within a straight cavity of the primary mass (see Fig.(1)). The particle undergoes impacts at the walls on either sides of the cavity, with a Newtonian coefficient of restitution $0 < r \leq 1$. The system is subjected to a harmonic base excitation, denoted by $e(t)$, with an amplitude E and a frequency ω . Let the coordinates $q_1(t)$ and

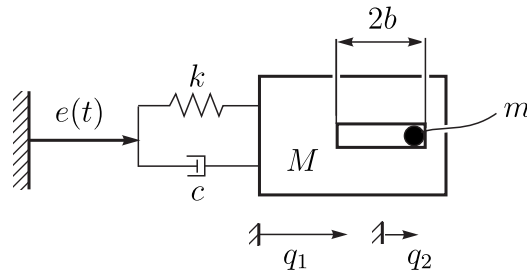


Fig. 1: Scheme of a LO coupled with a vibro-impact absorber (LO-VI NES).

$q_2(t)$ describe the absolute displacements of the primary mass M and secondary mass m , respectively. Contact with the cavity extremes exists if $|q_1 - q_2| = b$, where b is half the width of the cavity. In the following, we will only be interested in motions consisting of phases with no contact $|q_1 - q_2| < b$ with intermittent impacts when a collision occurs at contact. Persistent contact phases, during which contact is present during a non-zero time-interval, will not be considered. The non-impulsive motion is therefore described by the equation of motion

$$|q_1 - q_2| < b: \quad M\ddot{q}_1 + c\dot{q}_1 + kq_1 = ke(t) + c\dot{e}(t), \quad m\ddot{q}_2 = 0 \quad (1)$$

where k and c represent the stiffness and damping coefficients of the LO. The impulsive dynamics is governed by the Newtonian impact law and the conservation of linear momentum:

$$|q_1 - q_2| = b : \quad (\dot{q}_1^+ - \dot{q}_2^+) = -r (\dot{q}_1^- - \dot{q}_2^-) , \quad M\dot{q}_1^+ + m\dot{q}_2^+ = M\dot{q}_1^- + m\dot{q}_2^- . \quad (2)$$

The superscripts $(\cdot)^-$ and $(\cdot)^+$ denote the value at the time instant immediately before and after the impact, respectively, and the dots represent the differentiation with respect to the time t .

Following [5], we transform the equations of motion (1) and (2) into a normalised form, which allows the response analysis to be performed in a general framework. For this purpose, the following normalised parameters and quantities are introduced:

$$\epsilon = \frac{m}{M}, \quad G = \frac{E}{b\epsilon}, \quad \omega_0 = \sqrt{\frac{k}{M}}, \quad \Omega = \frac{\omega}{\omega_0}, \quad \lambda = \frac{c}{m\omega_0}, \quad \tilde{q}_1 = \frac{q_1}{b}, \quad \tilde{q}_2 = \frac{q_2}{b}, \quad \tau = \omega_0 t .$$

Next, barycentric coordinates $v = \tilde{q}_1 + \epsilon\tilde{q}_2$ and $w = \tilde{q}_1 - \tilde{q}_2$ that represent the displacement of the center of the mass and the internal displacement of the NES, respectively, are introduced. Substituting the new coordinates in (1) and (2) along with a harmonic base excitation function $e(t) = E \sin(\omega t)$ yields

$$\begin{aligned} \forall |w| < 1 : \\ v'' + \frac{\epsilon\lambda}{1+\epsilon}(v' + \epsilon w') + \frac{1}{1+\epsilon}(v + \epsilon w) &= \epsilon G \sin(\Omega\tau) + \epsilon^2 \Omega \lambda G \cos(\Omega\tau), \quad (3) \\ w'' + \frac{\epsilon\lambda}{1+\epsilon}(v' + \epsilon w') + \frac{1}{1+\epsilon}(v + \epsilon w) &= \epsilon G \sin(\Omega\tau) + \epsilon^2 \Omega \lambda G \cos(\Omega\tau), \\ \forall |w| = 1 : \quad v^+ = v^-, \quad w^+ = w^-, \quad v'^+ = v'^-, \quad w'^+ &= -rw'^-, \quad (4) \end{aligned}$$

where the prime symbol $(\cdot)'$ represents the differentiation w.r.t. the dimensionless time τ .

3 Multiple scales method

The first step in the analysis of the model described by the equations (3) and (4) requires the approximation of the solutions, whereby the corresponding quantities are uniformly expanded in power series of a small parameter. In this context, the mass ratio ϵ is used as a perturbation parameter and to define the new time scales necessary to carry out the analysis using the MSM [6]. The MSM exploits the fact that the motion can, approximately, be regarded to take place on two time scales: a slow and a fast scale. The oscillatory behavior is described by the fast time scale $\tau_0 = \tau$, and the decaying and shifting behavior is described by the slower time scale, denoted by $\tau_1 = \epsilon\tau$. Thus, the solutions v and w , considered to be functions of τ_0 and τ_1 , are expanded up to the first order:

$$\begin{aligned} v(\tau, \epsilon) &= v(\tau_0, \tau_1, \epsilon) \sim v_0(\tau_0, \tau_1) + \epsilon v_1(\tau_0, \tau_1) + \mathcal{O}(\epsilon^2), \\ w(\tau, \epsilon) &= w(\tau_0, \tau_1, \epsilon) \sim w_0(\tau_0, \tau_1) + \epsilon w_1(\tau_0, \tau_1) + \mathcal{O}(\epsilon^2). \end{aligned} \quad (5)$$

The substitution of the approximation (5) into the equations of motion (3) transforms the derived ODEs into PDEs according to:

$$\frac{d}{d\tau} = D_0 + \epsilon D_1, \quad \frac{d^2}{d\tau^2} = D_0^2 + 2\epsilon D_0 D_1 + \mathcal{O}(\epsilon^2), \quad \text{where } D_i = \frac{\partial}{\partial \tau_i}. \quad (6)$$

Next, the coefficients of the same ϵ -order in both sides of the obtained equations are set equal [7]. The approximated motions v_0 and w_0 between the impacts can be deduced and expressed using sine/cosine terms and a linear function that depend on the fast scale τ_0 , while the amplitudes and phases are expressed as functions of the slower scale τ_1

$$v_0(\tau_0, \tau_1) = C(\tau_1) \sin(\tau_0 + \theta(\tau_1)), \quad w_0(\tau_0, \tau_1) = v_0(\tau_0, \tau_1) + F(\tau_1)\tau_0 + D(\tau_1). \quad (7)$$

Determination of periodic motions: It is expected that the system exhibits periodic responses due to the harmonic periodic external excitation. Following [4, 7], the 1:1 internal resonance with two symmetric impacts per period is considered. This allows to express the linear term in w_0 using a nonsmooth sawtooth function as $w_0 = v_0 + B(\tau_1)\Pi(\tau_0 + \eta(\tau_1))$, where the k -th impact occurs at $\tau_{0,k}^c = \frac{\pi}{2} + k\pi - \eta$. The nonsmooth sawtooth function $\Pi(z)$ and its derivative $M(z)$ are defined as

$$\Pi(z) = \frac{4}{\pi} \sum_{k=1}^{\infty} \frac{(-1)^{k+1}}{(2k-1)^2} \sin((2k-1)z), \quad M(z) = \text{sign}(\cos(z)), \quad \forall z \neq \frac{\pi}{2} + k\pi. \quad (8)$$

Moreover, the quantitative nearness to primary resonance can be described by a dimensionless detuning parameter σ according to $\Omega = \frac{\omega}{\omega_0} = 1 + \sigma\epsilon$. The suppression of the secular terms in the dynamics of v_1 and w_1 results in a set of two first-order nonlinear ODEs that govern the modulation of the amplitude and phase of the solutions in the presence of 1:1 internal resonance between impacts [7]. Introducing the phase difference between the external excitation and the displacement of the center of mass, denoted by $\gamma = \theta - \sigma\tau_1$, as well as the phase difference between the external excitation and the internal displacement of the NES, denoted by $\psi = \eta - \sigma\tau_1$, the sought solutions can be written as

$$v_0 = C(\tau_1) \sin(\Omega\tau_0 + \gamma(\tau_1)), \quad w_0 = v_0 + B(\tau_1)\Pi(\Omega\tau_0 + \psi(\tau_1)), \quad (9)$$

and the resulting ODE system for the slow dynamics between the impacts, i.e. $|w_0| < 1$, is given by

$$\begin{aligned} D_1 C &= -\frac{1}{2} \left(\lambda C + \frac{4}{\pi} B \sin(\psi - \gamma) + G \sin(\gamma) \right), \\ D_1 \gamma &= -\frac{1}{2C} \left(-\frac{4}{\pi} B \cos(\psi - \gamma) + G \cos(\gamma) \right) - \sigma, \end{aligned} \quad (10)$$

while the jump in the amplitude B and phase η at a collision time-instant, i.e. $|w_0| = 1$, is governed by

$$\begin{aligned} B^+ &= rB^- + (1+r)C^- \cos(\Omega\tau_{0,k}^c + \gamma^-) M(\Omega\tau_{0,k}^c + \psi^-), \\ \psi^+ &= -\frac{B^-}{B^+} (\psi^- - k\pi) - \left(\frac{B^-}{B^+} + 1 \right) \Omega\tau_{0,k}^c + k\pi. \end{aligned} \quad (11)$$

The periodic solutions of (3) and (4) for 1:1 internal resonance with two symmetric impacts per period are approximately described using the slow variables (C, γ, B, ψ) by the equilibria of the system (10)-(11). Hence, a constant behavior at steady state for this type of motion can be characterized through the fulfillment of the following three conditions. In the upcoming derivations, the subscript $(\cdot)_{ss}$ denotes the constant values of the variables at steady state.

Condition 1: Internal 1:1 resonance with two symmetric impacts per period: For this type of steady state, the contact condition and the corresponding impact relations can be reformulated. Substituting the collision time instant $\tau_{0,k}^c = \frac{1}{\Omega} (\frac{\pi}{2} + k\pi - \psi)$ into the impact condition $|w_0| = 1$ and the impact laws (11), while assuming a constant amplitude B during this type of motion, delivers two conditions that can be combined to obtain a relationship between the LO's oscillation amplitude C and the velocity B of the NES

$$C^2 = R^2 B^2 + \left(1 - \frac{\pi}{2} B\right)^2 \quad \text{with} \quad R = \frac{1-r}{1+r}. \quad (12)$$

Equation (12) describes a 2D manifold in the slow variables configuration space, called *the slow invariant manifold (SIM)*, which only depends on the coefficient of restitution r .

Conditions 2 and 3: Constant amplitude and constant phase at steady state: The fulfillment of both conditions requires considering the slow dynamics of the variables C and γ . Consequently the right-hand side of the ODEs in (10) must vanish to guarantee a constant behavior over time.

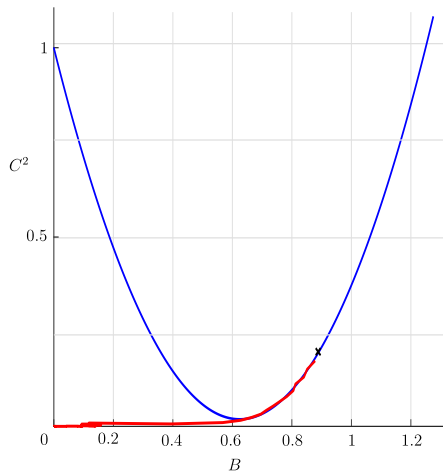


Fig. 2: Free resonant motion of the VI NES on the SIM for $r = 0.65$. The black cross represents the equilibrium attained with the PLL for $G = 1.1$.

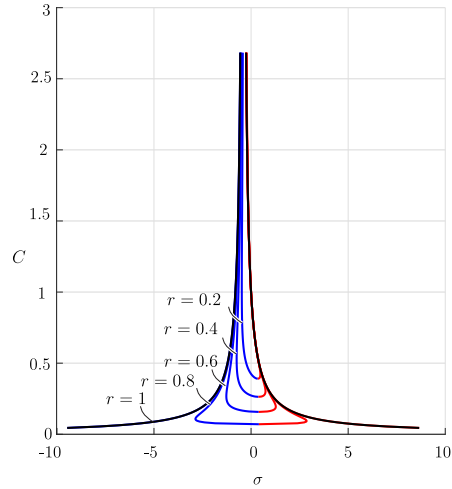


Fig. 3: Backbone curves for different values of r . The black lines correspond to $r = 1$.

Description of the system's flow on the SIM: Fulfillment of all conditions: The two above-mentioned conditions describe the steady-state motion on the SIM. For an initial condition which is not on the SIM follows a short rapid motion to the SIM at the time-scale τ_0 , followed by a slow motion along the SIM possibly to a steady-state. Here, we will be interested in the slow quasi-static motion along the SIM at the time-scale τ_1 . After rearranging (10), inserting the inelastic impact conditions and introducing a new variable $\tilde{C} = C^2$, the ODE system that describes the time variation w.r.t. the slow time variable τ_1 along the SIM is given by

$$\begin{aligned} D_1 \tilde{C} &= -\lambda \tilde{C} - \frac{4}{\pi} R B^2(\tilde{C}) - G \sqrt{\tilde{C}} \sin(\gamma), \\ D_1 \gamma &= \frac{1}{\tilde{C}} \frac{2}{\pi} B(\tilde{C}) \left(1 - \frac{\pi}{2} B(\tilde{C})\right) - \frac{G}{2\sqrt{\tilde{C}}} \cos(\gamma) - \sigma. \end{aligned} \quad (13)$$

Since the investigation of the steady state solutions occurs on the SIM, the amplitude B can be expressed as a function of the amplitude \tilde{C} , namely,

$$B(\tilde{C}) = B_{\min} \pm \sqrt{\frac{\pi}{2} B_{\min} \left(\tilde{C} - \tilde{C}_{\min}\right)} \quad \text{with} \quad B_{\min} = \frac{\frac{\pi}{2}}{R^2 + \frac{\pi^2}{4}}, \quad \tilde{C}_{\min} = \frac{R^2}{R^2 + \frac{\pi^2}{4}}.$$

The determination of the equilibria for the system above follows from setting the right-hand side of (13) to zero or, equivalently, solving the equations

$$\begin{aligned} -G \sqrt{\tilde{C}_{ss}} \sin(\gamma_{ss}) &= k_1 \tilde{C}_{ss} \pm k_2 \sqrt{\tilde{C}_{ss} - \tilde{C}_{\min}} + k_3, \\ G \sqrt{\tilde{C}_{ss}} \cos(\gamma_{ss}) &= k_4 \tilde{C}_{ss} \pm k_5 \sqrt{\tilde{C}_{ss} - \tilde{C}_{\min}} + k_6 \end{aligned} \quad (14)$$

with the coefficients

$$\begin{aligned} k_1 &= \lambda + \frac{8}{\pi^2} R B_{\min}, & k_2 &= \frac{8}{\pi} R B_{\min} \sqrt{\frac{2}{\pi} B_{\min}}, \\ k_3 &= \frac{4}{\pi} R B_{\min} \left(B_{\min} - \frac{2}{\pi} \tilde{C}_{\min}\right), & k_4 &= -\frac{4}{\pi} B_{\min} - 2\sigma, \\ k_5 &= \frac{4}{\pi} \sqrt{\frac{2}{\pi} B_{\min}} (1 - \pi B_{\min}), & k_6 &= \frac{4}{\pi} B_{\min} \left(1 - \frac{\pi}{2} B_{\min} + \tilde{C}_{\min}\right). \end{aligned} \quad (15)$$

The equilibria from (14) describe the steady state response regime of the original system from (1)-(2) in the state of 1:1 resonance. Therefore, the SIM can be perceived as the possible set of equilibria that could satisfy the 1:1 resonance with two symmetric impacts per period at steady state. Thus, the study of the evolution of the flow on the SIM and the existence of a corresponding equilibrium on the SIM give an insight into the behavior of the original system and its modal motion. The stable and unstable regions of the SIM have been established and can be found in [5, 7].

4 Nonlinear mode identification

In this section, the analysis is pushed further to investigate and determine the modal properties of the LO VI-NES using the results from the previous section.

In a first step towards modal identification, despite the complexity of the system's dynamics, the phase resonance condition can be exploited as a straightforward extension of the linear theory. The main idea is to determine the frequency at which the response amplitude is at its maximum value. The resonance frequency Ω_R is characterized by the parameter σ_R through $\Omega_R = 1 + \sigma_R \epsilon$. Considering the steady state amplitude $\tilde{C}_{ss} = \tilde{C}_{ss}(\sigma)$ to be a function of σ , the resonance condition is given by

$$\left. \frac{\partial \tilde{C}_{ss}}{\partial \sigma} \right|_{\sigma=\sigma_R} = 0, \quad \text{and} \quad \left. \frac{\partial^2 \tilde{C}_{ss}}{\partial \sigma^2} \right|_{\sigma=\sigma_R} < 0. \quad (16)$$

For convenience, we use in the next derivation the notation $(\cdot)'$ for differentiation w.r.t. σ at $\sigma = \sigma_R$. Using the resonance condition $\tilde{C}'_{ss} = 0$, the steady state condition (14) can be differentiated with respect to σ , to yield

$$G\sqrt{\tilde{C}_{ss}}\gamma'_{ss} \cos(\gamma_{ss}) = 0, \quad G\sqrt{\tilde{C}_{ss}}\gamma'_{ss} \sin(\gamma_{ss}) = -k'_4 \tilde{C}_{ss} \neq 0. \quad (17)$$

and therefore, $\gamma'_{ss} \neq 0$, $\sin(\gamma_{ss}) \neq 0$ and $\cos(\gamma_{ss}) = 0$. Moreover, from (13) we can deduce that $\sin(\gamma_{ss}) < 0$, which yields the extremum condition

$$\gamma_{ss} = -\frac{\pi}{2} + 2p\pi, \quad p \in \mathbb{Z}. \quad (18)$$

Consequently, similar to linear systems, the identification of a nonlinear mode of the vibro-impact system requires approximately a phase difference of $\frac{\pi}{2}$ between the external excitation and the displacement.

Inserting the phase resonance condition (18) into (14) yields

$$G\sqrt{\tilde{C}_{ss,R}} = k_1 \tilde{C}_{ss,R} \pm k_2 \sqrt{\tilde{C}_{ss,R} - \tilde{C}_{\min}} + k_3, \quad (19)$$

$$0 = k_4 \tilde{C}_{ss,R} \pm k_5 \sqrt{\tilde{C}_{ss,R} - \tilde{C}_{\min}} + k_6, \quad (20)$$

Equation (19) defines the relation between the steady state amplitude at resonance $\tilde{C}_{ss,R}$ and the external excitation level G . Equation (20) depends on $k_4 = k_4(\sigma)$ and can be reformulated to express the detuning parameter σ_R (as well as the frequency Ω_R) as a function of the steady state amplitude and the system parameter r according to

$$\sigma_R = \frac{1}{2\tilde{C}_{ss,R}} \left(\pm k_5 \sqrt{\tilde{C}_{ss,R} - \tilde{C}_{\min}} + k_6 \right) - \frac{2}{\pi} B_{\min}. \quad (21)$$

Equation (21) describes the backbone curve for the amplitude response of the considered nonlinear system: Figure (3) depicts the obtained curves for different values of the coefficient of restitution r . In a second step towards the modal identification, a verification of the obtained modal lines is pursued via the extended periodic motion concept (EPMC), a modal approach developed by Krack [16], where the isolation of a NM is performed using a controlled external excitation. The results of this approach will not be discussed in this work. However, we were able to show that, for the studied system, the EPMC is equivalent to the phase resonance condition $\gamma_c = -\frac{\pi}{2}$, if terms up to the first-order $\mathcal{O}(\epsilon)$ are considered.

5 Numerical experiments and simulation results

The main focus of this section lies on the identification of the backbone curve of the considered NM from the resonance decay response of the system combined with a Phase-Locked-Loop (PLL)[2, 3]. This procedure relies on the invariance property of the NM, as it represents the main characteristic that unifies the different definitions of NMs. The PLL will be used to control the response of the forced system to attain a specific type of resonance, namely 1:1 internal resonance with two symmetric impacts per period. When the NM is reached, i.e. the equivalent slow flow is on the SIM, the controller is turned off and the decaying response along the NM and the corresponding SIM is monitored and analysed. The introduced modal approaches are implemented and compared with direct numerical simulations results of the nonlinear system (3) and (4). The numerical values used for the simulation are taken from [7]. The tuning parameters of the implemented PLL-controller are chosen heuristically in such a way that the stability, the convergence as well as a minimal phase error over time are guaranteed. The simulations are carried out for different levels of external excitation followed by analysis and comparison of the results. The observations concern essentially the location of the computed equilibria.

For a low level of forcing, the system (13) possesses two equilibria. One lies on the left branch of the SIM, characterized by an amplitude B_{ss} below the NES activation threshold B_{min} , and the second equilibrium is situated on the low side of the right branch. However, the computed equilibria for medium or high level of excitation are always located on the right branch of the SIM and are characterised by a much higher amplitude C_{ss} and an amplitude B_{ss} above the activation threshold of the NES. It has also been noticed that the PLL does only converge towards the equilibria situated in the low right side of the SIM, suggesting that it only permits the generation of stable steady state solutions, and therefore attains only stable regions of the nonlinear mode. This suggestion is actually confirmed by the results presented in [5, 7], where the stable areas of the SIM have been established.

Based on this first interpretation, the developed approach is used to identify the stable parts of the analytically determined backbone curve. First, the closed loop system is simulated long enough for the solution to attain a stable steady state. The analytical and numerical values of this first step are compared in Fig.(4). It can be clearly seen that the PLL solution converges toward the equilibrium that satisfies the activation threshold condition. Next, the system's input is removed and the decaying evolution of the flow along the SIM is monitored. With an absent external excitation, the oscillation's amplitude decreases until the VI NES is completely inactive. The flow of the free resonant response is depicted in Fig.(2). The regime of 1:1 resonance with two symmetric impacts per period is maintained despite the decreasing oscillation's amplitude C . Subsequently, the velocity of the VI NES decreases until the activation threshold is no longer satisfied, at which point the flow leaves the SIM and the internal impacts of the NES are no longer synchronized and vanish over time. The damping effect due to the NES internal impacts ceases, and the decrease of the LO amplitude

is caused essentially by the linear damping of the structure. The oscillation's amplitude and frequency are directly evaluated from the free resonant response. Lastly, the numerically estimated backbone curve, describing the dependency between the amplitudes $\hat{C}_{i,\max}$ and their corresponding frequencies through the detuning parameter $\hat{\sigma}_{i,\max}$, is compared to the analytic prediction from (21). The estimated modal line is shown in Fig.(5), depicting the identified stable branch of the backbone curve and confirming the analytical results.

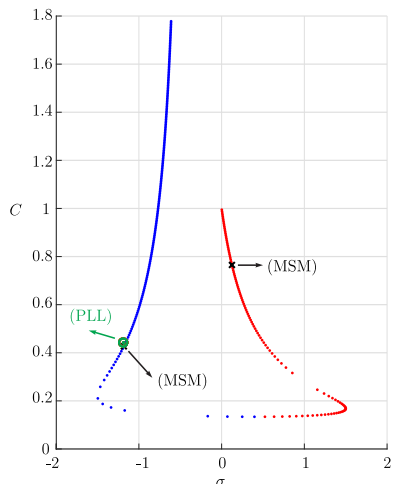


Fig. 4: Comparison of the analytically and numerically estimated amplitude and the corresponding frequency for $G = 1.1$.

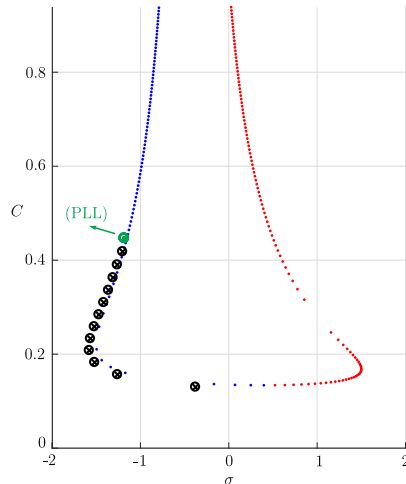


Fig. 5: Backbone curve for $r = 0.65$. The green point represents the starting point attained with the PLL for $G = 1.1$. The black crossed circles correspond to the estimated values from the free resonant response.

6 Conclusion

The dynamics of a linear oscillator coupled with a VI NES and subjected to a harmonic excitation in the vicinity of resonance is investigated theoretically and numerically. Using the MSM under the assumption of a very small mass ratio, a relationship between the motion of the main system and the VI NES velocity is established. The expression of the 2D manifold in the slow variables space is determined and the relation between its topology and the predicted system's response is investigated. It is shown that the resonance frequency and the corresponding resonance amplitude are closely related to the position of the fixed points on the SIM. The developed analytical investigation is pushed further to extract the modal properties of the system. The resonance condition for the system is derived and used to determine a closed-form description of the system's

considered backbone curve. The verification of the obtained results is carried out numerically. The backbone curve of the considered nonlinear mode is identified using the resonance decay response of the system combined with a PLL. The presented results of the numerical simulations agree with the theoretical findings. Further exploitation of these results will concern their extension and application to more complex structures with possible mode interaction or the investigation of different response regimes around the SIM, which may provide a deeper understanding of the VI-NES dynamics.

References

1. G. Kerschen, M. Peeters, J.C. Golinval, A.F. Vakakis (2009) Nonlinear normal modes, Part I: A useful framework for the structural dynamicist. *J. Mechanical Systems and Signal Processing* **23**:170-194.
2. S. Peter, R. Riethmüller, R.I. Leine (2016) Tracking of backbone curves of nonlinear systems using phase-locked-loops. *Nonlinear Dynamics* **1**:107-120.
3. Best, Roland E (2007) Phase-locked loops: design, simulation, and applications. *McGraw-Hill Education*.
4. O.V. Gendelman, A. Alloni, (2015) Dynamics of forced system with vibro-impact energy sink. *J. of Sound and Vibration* **358**:301-314.
5. T. Li, S. Seguy, A. Berlioz (2016) Dynamics of cubic and vibro-impact nonlinear energy sink: analytical, numerical, and experimental analysis. *J. Mechanical Systems and Signal Processing* **138**:031010.
6. A. Nayfeh (2011) Introduction to perturbation techniques. *John Wiley & Sons*
7. E. Gourc, G. Michon, S. Seguy, A. Berlioz (2015) Targeted energy transfer under harmonic forcing with a vibro-impact nonlinear energy sink: analytical and experimental developments. *Journal of Vibration and Acoustics* **137** (3).
8. O. V. Gendelman (2012) Analytic treatment of a system with a vibro-impact nonlinear energy sink. *Journal of Sound and Vibration* **331**(21):4599-4608.
9. T. Li, S. Seguy, A. Berlioz (2017) Optimization mechanism of targeted energy transfer with vibro-impact energy sink under periodic and transient excitation. *Nonlinear Dynamics* **87**(4):2415-2433.
10. T. Li, S. Seguy, A. Berlioz, E. Gourc (2015) Analysis of a vibro-impact nonlinear energy sink: theoretical and numerical developments. In *Congrès français de mécanique. AFM, Association Française de Mécanique*
11. E. Gourc, G. Michon, S. Seguy, A. Berlioz (2014) Experimental investigation and design optimization of targeted energy transfer under periodic forcing. *Journal of Vibration and Acoustics* **136**(2).
12. O.V. Gendelman, A. Alloni, (2016) Forced system with vibro-impact energy sink: chaotic strongly modulated responses. *Procedia IUTAM* **19**(1):53-64.
13. T. Li, S. Seguy, A. Berlioz (2017) On the dynamics around targeted energy transfer for vibro-impact nonlinear energy sink. *Nonlinear Dynamics* **87**(3):1453-1466.
14. J. M. Londoño, S. A. Neild, J. E. Cooper (2015) Identification of backbone curves of nonlinear systems from resonance decay responses. *Journal of Sound and Vibration* **348**:224-238.
15. L. Renson, A. Gonzalez-Buelga, D. A. W. Barton, S. A. Neild (2016) Robust identification of backbone curves using control-based continuation. *Journal of Sound and Vibration* **367**: 145-158.
16. M. Krack (2015) Nonlinear modal analysis of nonconservative systems: extension of the periodic motion concept. *Computers & Structures* **154**: 59-71.